2(mix)-P

Airglow and Auroral Expedition

Aboard the CV 990 Aircraft

Final Report: NASA Grant NGR-06-003-110

This grant supported participation by the University of Colorado in the NASA - Airborne Auroral expedition in November-December 1969, analysis of the data obtained during the experiment, and theoretical studies relevant to interpretation of the results.

Instrumentation

Observations were made with a scanning spectrometer and a single channel photometer. The scanning spectrometer is a half-meter Fastie-Ebert instrument. The grating has a 3000 Å blaze and a thermoelectrically cooled EMR 543E photomultiplier tube was used. Interchangeable cams provided the capability to scan over wavelength ranges of approximately 1000, 500, 250, 100 and 50 Angstroms. These ranges were all used during the course of the experiment. The duration of a single scan could be 100, 50, 25 and 12½ seconds, the choice being determined by the brightness and morphology of the aurora, as well as the wavelength interval under investigation and the spectral resolution. Observations were made in the wavelength interval between 3100 and 6300 Angstroms with emphasis on the near ultraviolet region to take advantage of the optical characteristics of the spectrometer and the altitude of the aircraft.

The spectrometer and photometer veiwed through quartz windows. Other instruments on board the aircraft observed in the visible and near infrared portions of the spectrum.

The single channel photometer was mounted coaxially with the spectrometer. It recorded the N_2^+ IN (λ4278) radiation and served to monitor the temporal changes of the auroral brightness during a spectral scan. The electrometer amplifiers have a D.C. 0-5 Volt output, linear response for the spectrometer and quasi-logarithmic for the photometer. Analog spectrometer and photometer signals were recorded on magnetic tape, together with a time signal, reference oscillator signal and fiducial mark. A voice channel contains the conversations between experimenters and flight director as well as comments on auroral conditions by the visual observer.

Calibration

The slit width of the spectrometer is adjustable; the resolution, $\Delta\lambda/\lambda$, is shown in Figure 1 as a function of slit setting (roughly corresponding to thousandths of an inch).

The absolute intensity calibration as a function of wavelength of the spectrometer and photometer was obtained in the laboratory using a black body source of radiation. Another calibration was made in the hanger at Ft. Churchill using the Johns Hopkins University source. The results of

the two calibrations are shown in Figure 2. The Ft. Churchill procedure also served as a cross calibration check amongst the various optical instruments on board the aircraft. The wavelength interval scanned with each of the four cams is determined by the starting position of the grating as controlled by a notched cam permanently mounted on the grating shaft. The notches are numbered from 1 to 53; Figure 3 gives the starting wavelength as a function of notch position. The wavelength interval covered by each cam is about 5% less than the nominal value, e.g. the 1000 Å cam only scans about 950 Å, due to the flyback portion of the cycle.

The absolute calibration of the λ4278 photometer is shown in Figure 4. The integrated area under the filter transmission curve is 2.9 Å and the width of the pass band at half maximum is 8.8 Å.

The Observational Data

The value of this expedition rested in the complement of instruments that was used to study the aurora. Optical detectors covered the wavelength range from the near ultraviolet (about 3100 Å) to the near infrared (about 2 μ). The spectrometers and photometers were supplemented by all sky cameras, a riometer and a magnetometer. The Colorado spectrometer was optimized in the near ultraviolet region of the spectrum but could be operated to a long wavelength

limit determined by the second order overlap.

Observations were usually made in the zenith, through a quartz window, and occasionally through a side window, corresponding to a 75° zenith angle when the aircraft was in level flight. The available data for each flight are listed in the spectrometer log given below. Sufficient details are given to inform other airborne experimenters of the information obtainable from the half meter spectrometer tapes. The first column lists the flight number and the corresponding date is given in the second column. The time (U.T.) when some change in setting was made is shown next. The nominal wavelength interval that was scanned is shown in the fourth column, and the duration of the scan is listed next. The notched cam position is indicated in column six and the slit width is shown in column seven. Column eight indicates whether the observation was made in the zenith or out the side window and miscellaneous comments appear last. For example, during flight 5, on 29 November 1969, beginning at 0250 UT the 500 Å cam was used with the 100 sec scan motor. The notch was set at position 52 so that the wavelength interval was between 3840 and 3360 Å (Figure 3). In this wavelength interval there are 2PG and V-K bands of N_2, bands of N_2^+ and the NI line at 3460 Å. The slit setting was 20, corresponding to an average 3 Å pass band (Figure 1), the

Auroral Airborne Expedition, 1969

HALF METER SPECTROMETER LOG

Flight No	Date	Time, U.T.	Cam(Å)	Motor (sec)	Position	Slit	Window	Comments
1	19 Nov	0600	1000	100	14	wide	Zenith	
2	24 Nov	1030	1000	100	49	20	Zenith	
		1045	250	50	34	20	Zenith	
		1140	1000	100	49	20	Zenith	
		1149				13	Zenith	
3	26 Nov	0055	250	50	34	20	Zenith	
		0155	250	50	34	20	Side	
		0200	250	50	34	20	Zenith	
		0211	1000	25	44	13	Zenith	
		0219	1000	25	44	4½	Zenith	
		0331	1000	25	44	13	Zenith	
		0457	1000	25	49	4½	Zenith	
		0522	1000	25	49	9		
		0556	1000	25	49	4½	Zenith	
4	27 Nov	0105	50	25	12	9	Side	
		0113	50	25	12	13	Side	
		0120	50	25	34	13	Zenith	
		0131	50	25	21	13	Zenith	
		0202	1000	50	40	13	Zenith	
		0327	2000	50	28	13	Zenith	
		0503	1000	50	21	13	Side	
		0512	1000	50	49	9	Side	
		0522	1000	50	1	20	Side	
		0526	1000	50	2	20	Side	
		0528	1000	50	3	20	Side	

Flight No	Date	Time, U.T.	Cam(Å)	Motor (sec)	Position	Slit	Window	Comments
		0534	1000	50	49	20	Zenith	
		0544						Shut down
5	29 Nov	0225	250	100	34	20	Zenith	
		0250	500	100	52	20	Zenith	OGO intercept
		0307	500	100	52	13	Zenith	ATS grid
		0628	50	50	14	13	Zenith	
		0650	50	50	14	13	Side	
		0700	50	50	14	13	Zenith	
		0720	50	50	several	13	Zenith	Cam tests
6	3 Dec	0520	1000	50	49	13	Zenith	
		0710	50	12½	28	13	Zenith	
		0838	1000	50	49	13	Zenith	
		1025						Shut down
7	4 Dec	0454	1000	50	49	13	Zenith	
		0505	1000	50	49	20	Zenith	
		0608	1000	50	49	13	Zenith	
		0748	1000	50	49	20	Zenith	
		0912						Shut down
8	5 Dec	0616	1000	50	49	20	Zenith	
		0815	50	12½	51	9	Zenith	
		0823	50	12½	51	5	Zenith	
		1130						Shut down
9	7 Dec	0527	50	50	34	9	Zenith	
		0602	1000	100	49	9	Zenith	
		0612	1000	100	49	13	Zenith	
		0720	1000	25	49	13	Zenith	
		1030						Shut down
10	8 Dec	0758	2000	100	1	13	Zenith	
		0814	2000	100	35	13	Zenith	
		0852	2000	100	1	13	Side	
		0941	2000	100	35	13	Zenith	
		1042	2000	100	34	13	Zenith	

Flight No	Date	Time, U.T.	Cam(Å)	Motor (sec)	Position	Slit	Window	Comments
		1112	2000	100	34	13	Side	
		1152	2000	100	34	13	Zenith	
		1225	2000	100	1	13	Side	
		1237	2000	100	34	13	Side	
		1252						Shut down
11	11 Dec	1911	2000	100	34	13	Zenith	Twilight
		1922	2000	100	33	13	Zenith	
		1948	2000	100	33	20	Zenith	
		2146	2000	100	33	9	Zenith	
		2159	2000	100	33	13	Zenith	
		2251						Shut down
12	13 Dec	0644	1000	100	49	20	Zenith	
		1039	1000	100	49	4½	Zenith	Twilight
		1107	1000	100	49	1	Zenith	
		1140						Shut down
13	14 Dec	0547	1000	100	49	20		
		0936	1000	100	49	9		
		0949	1000	100	49	4½		
		1005	1000	100	49	2	Zenith	
		1015						Shut down
14	16 Dec	0216	1000	50	49	20	Zenith	
		0219	1000	50	49	13	Zenith	
		0433	1000	50	49	20	Zenith	
		0745	1000	50	49	9	Zenith	
		0810						Shut down
15	18 Dec	0820	100	50	44	30	Zenith	
		0833	100	50	44	35	Zenith	
		0846	1000	100	49	20	Zenith	
		1342						Shut down

observations were made in the zenith, and these settings were used during an OGO-6 overpass.

The photometer monitored only the N_2^+ λ4278 band, viewing in the same direction as the spectrometer.

Flight details, auroral conditions, aircraft parameters, satellite intercepts and special circumstances appear in various bulletins issued by the Airborne Science Office in connection with the expedition, from data collected by all the experimenters and the general flight log. These bulletins, together with the experimenters' logs, provide the details of the auroral observations obtained during the expedition.

Analysis of the Data

It was noted previously that the data were analog recorded on seven channel magnetic tape. It was planned to digitize the data so that successive scans could be added as required by the signal to noise ratio. We have not had access to the necessary computer hardware for this mode of data analysis, and have resorted to direct readout of selected scans from the tape on to a chart recorder. A sample scan is shown in Figure 5. Each tape contains one or more voltage calibration runs so that the absolute intensity of the spectral features shown may be obtained.

Some 3000 spectra were recorded most of which require signal averaging (addition of scans) for analysis. A proposal for further reduction and analysis of our data is given later in this report.

In the meantime a theoretical study was carried out that underlies the interpretation, not only of the half meter spectrometer data, but of all the photometric-spectroscopic results obtained on the airborne expeditions. Briefly, the theory relates observed spectroscopic parameters to the characteristics of the bombarding auroral particle fluxes. There are several excitation processes that operate to produce the various spectral emissions. Some excited states are collisionally quenched at low altitude if their radiative lifetime is long compared to the quenching rate. Three commonly recorded auroral radiations are the N_2^+ IN band at 4278 Å and the OI lines at 5577 Å and 6300 Å. The ratios $\lambda 6300/\lambda 4278$ and $\lambda 5577/\lambda 4278$ as a function of the $\lambda 4278$ emission rate can be used to infer the flux $\mathcal{J}$, and spectral hardness α(keV) of the bombarding electron flux. The results of our computations are shown in Figures 6 and 7 and 8 (taken from a manuscript in preparation).

The validity of this procedure can be tested by comparison with appropriate satellite measurements of precipitating particle fluxes. Indirect verification of the electron flux

can be obtained by computing excitation rates of several auroral spectral features, e.g. the N_2 2PG system, and OI lines. Such a study has been done for a coordination between the CV 990 and OGO-4 from observations obtained during the 1968 expedition (Sharp and Rees, 1972). For this one occasion predicted and observed emission rates agree reasonably well, lending confidence to the theoretical formulation.

Proposal for Future Work

In order to optimize future data reduction and analysis it is suggested that the observations obtained with the Johns Hopkins spectrometer and photometer, the Alaska photometers, and the Colorado spectrometer and photometer be analyzed together. One individual would become expert in handling the data with help and guidance from the investigators who conducted the respective experiments. It is suggested that the work be carried out in Alaska, where the all-sky-camera films are available and where there is a large group interested in and working on auroral phenomena. This possibility has already been discussed by the concerned individuals and agreement has been reached. The formal proposal will originate from the University of Alaska.

Publications

"Latitude Distribution of the Night Airglow," W. E. Sharp and M. H. Rees, J. Geophys. Res. 75, 4894, 1970.

"The Auroral Spectrum Between 1200 and 4000 Angstroms," W. E. Sharp and M. H. Rees, J. Geophys. Res. 77, 1810, 1972.

"Characteristics of Auroral Electron Spectra as Determined by Spectroscopic Ratios of Emission Rates." (In preparation)

Figure Captions

Figure 1 Spectral resolution of the half meter spectrometer as a function of the slit width setting.

Figure 2(a) Relative sensitivity of the half meter spectrometer as a function of wavelength according to the Colorado laboratory calibration (solid curve) and the Johns Hopkins field calibration (dashed curve).

(b) The relative sensitivity must be multiplied by the quantity shown to obtain the absolute response of the spectrometer at various slit settings.

Figure 3 Setting of the notched cam corresponding to the long wavelength beginning of a spectral scan. The curve shows an average for the various cams that were used.

Figure 4 Absolute calibration of the N_2^+ ING (λ4278) photometer. The uncooled unit has a noise equivalent signal of about 25 rayleighs.

Figure 5 Data reproduced from magnetic tape comprising the time interval from 0730 to 0731 U.T. on 16 December during Flight 14. From top to bottom are shown the photometer trace, the

spectrometer trace with a 10 fold amplification, the spectrometer with a 100 fold amplification, and the time signal. The fiducial, A. C. clock, and voice channels are not shown. The calibration appropriate to each channel has been superposed on the trace.

Figure 6 The ratio of emission rates of the OI (λ6300) line to the N_2^+ ING (λ4278) band as a function of the latter for a range of precipitating electron fluxes with energy distribution E exp (-E/α) where α(keV) is the characteristic energy.

Figure 7 The ratio of emission rates of the OI (λ5577) line to the N_2^+ ING (λ4278) band as a function of the latter for a range of precipitating electron fluxes with energy distribution E exp (-E/α) where α(keV) is the characteristic energy.

Figure 8 Precipitating electron flux associated with a range of λ4278 emission rates for a range of energy distributions of characteristic energy α(keV).

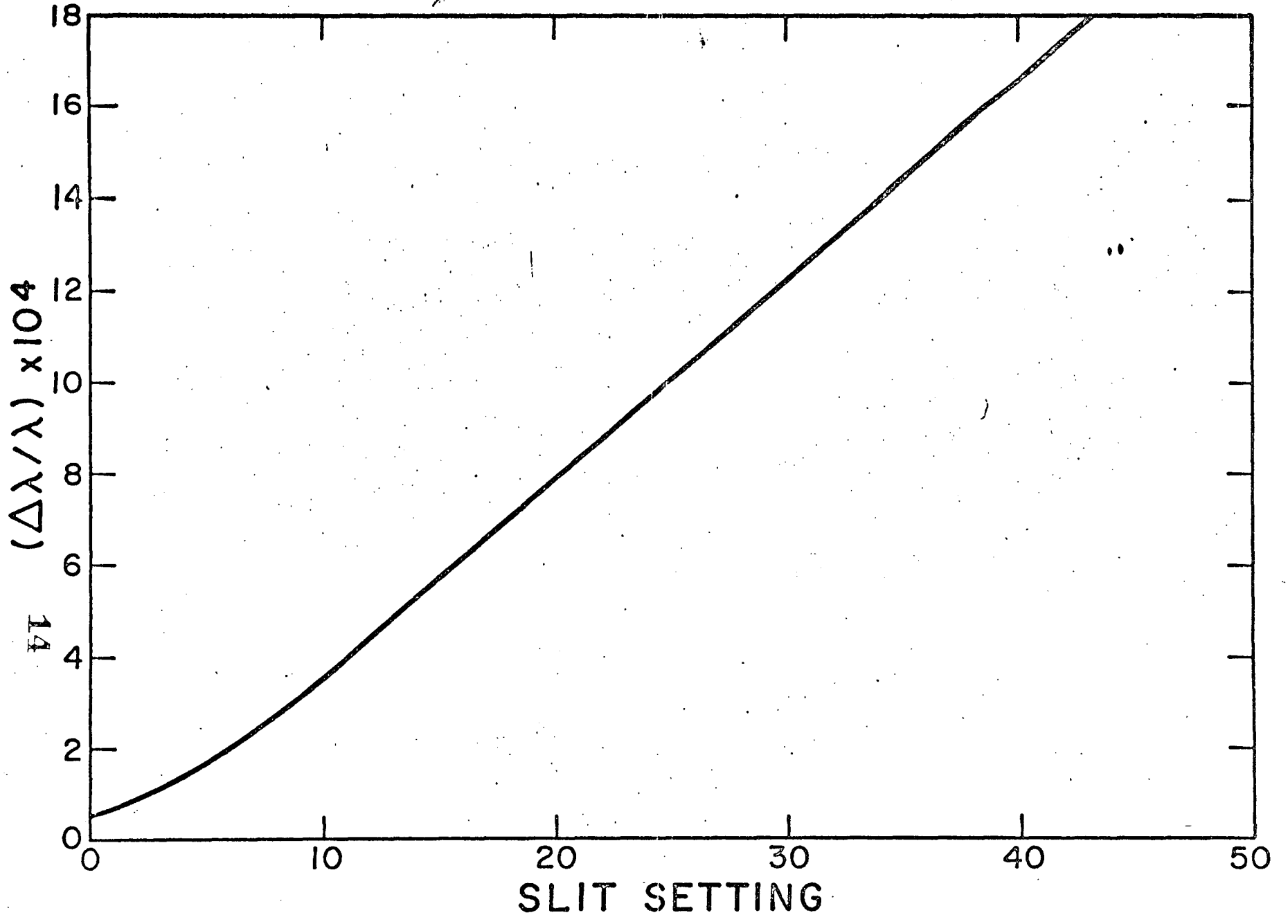
18
16
14
12
10
8
6
4
2
0
0
10
20
30
40
50
SLIT SETTING
(Δλ/λ) x104

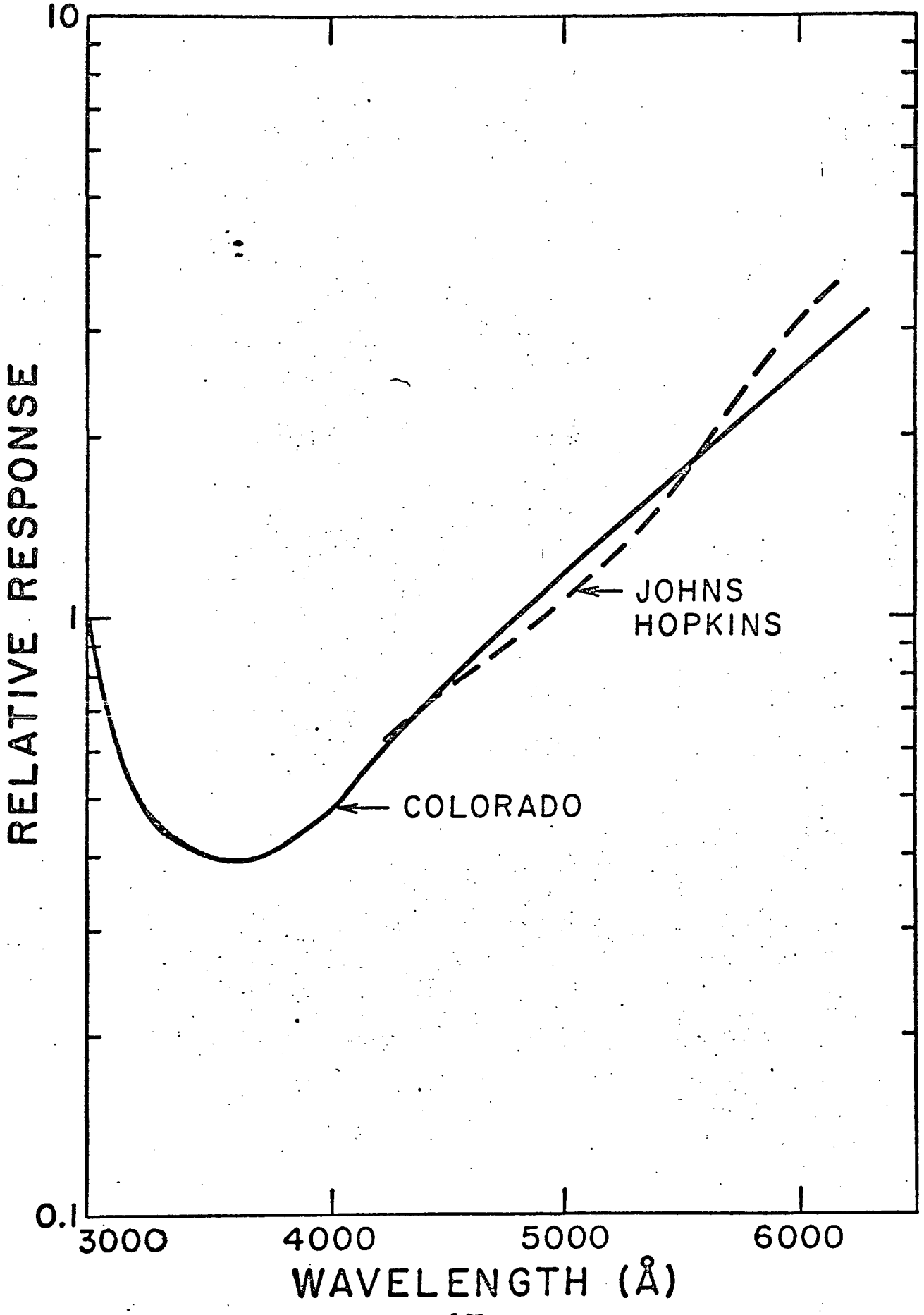
10
1
0.1
RELATIVE RESPONSE
JOHNS
HOPKINS
COLORADO
3000
4000
5000
6000
WAVELENGTH (Å)

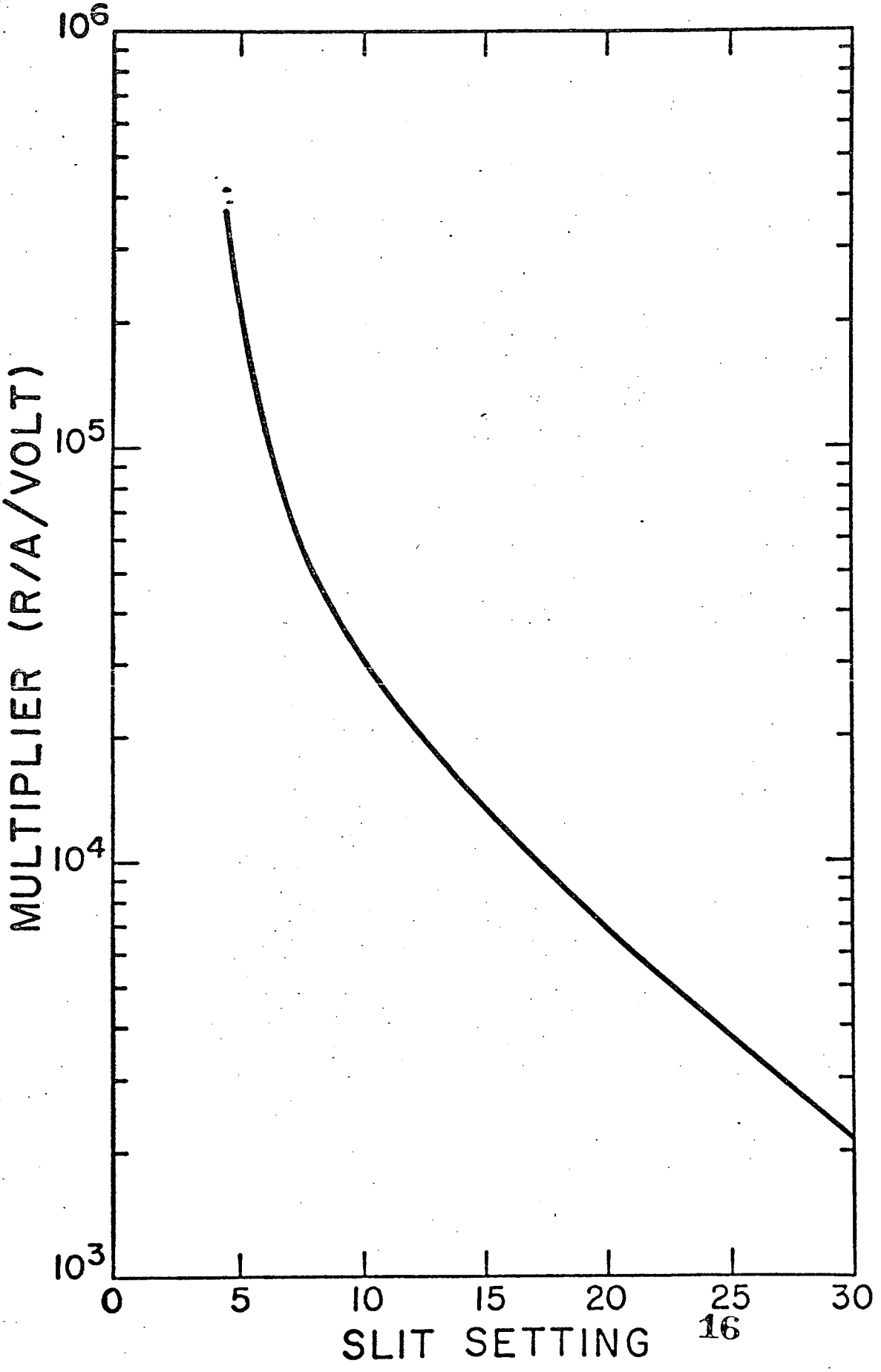
10^6
10^5
10^4
10^3
MULTIPLIER (R/A/VOLT)
0
5
10
15
20
25
30
SLIT SETTING

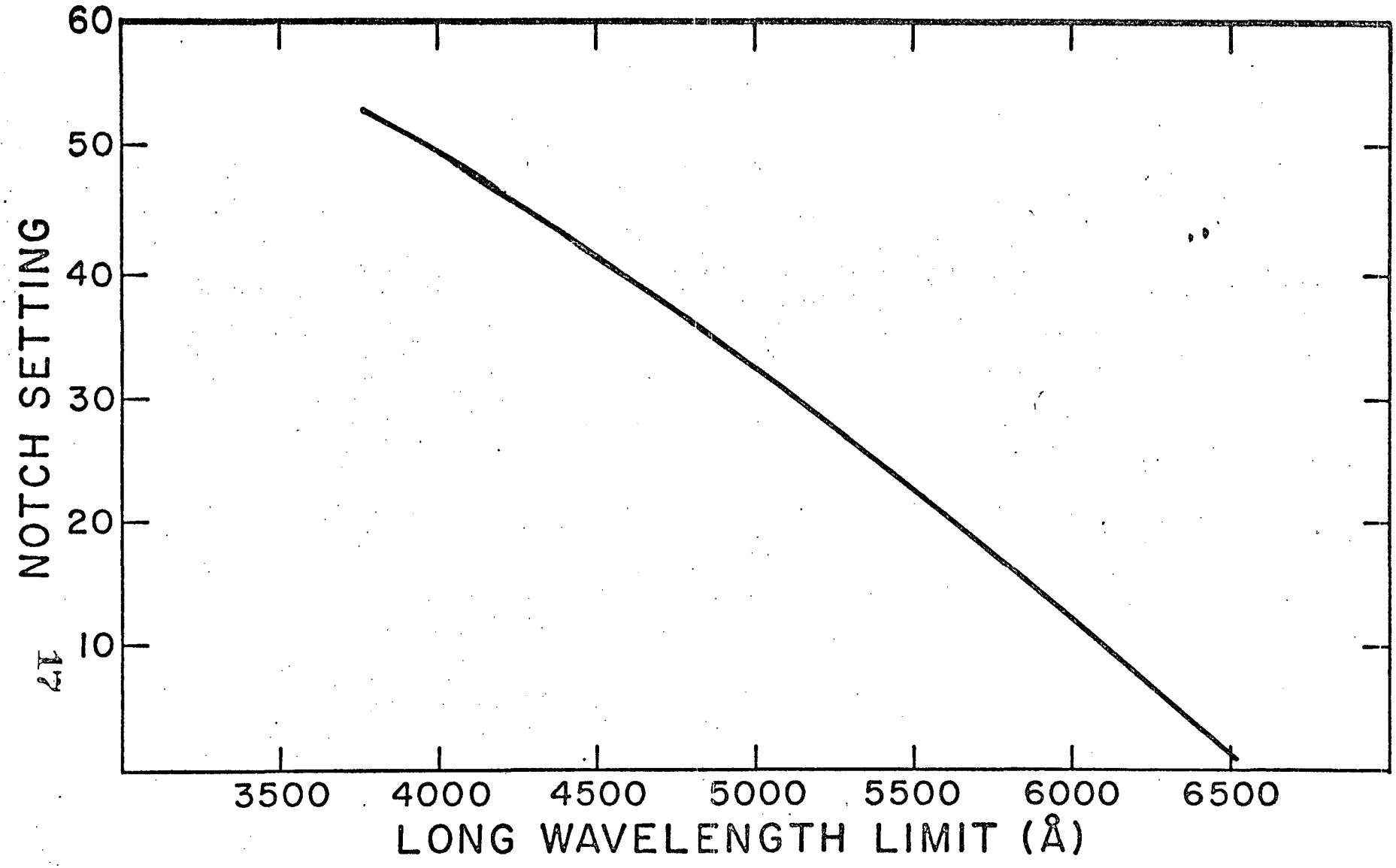
60
50
40
30
20
10
NOTCH SETTING
3500
4000
4500
5000
5500
6000
6500
LONG WAVELENGTH LIMIT (Å)

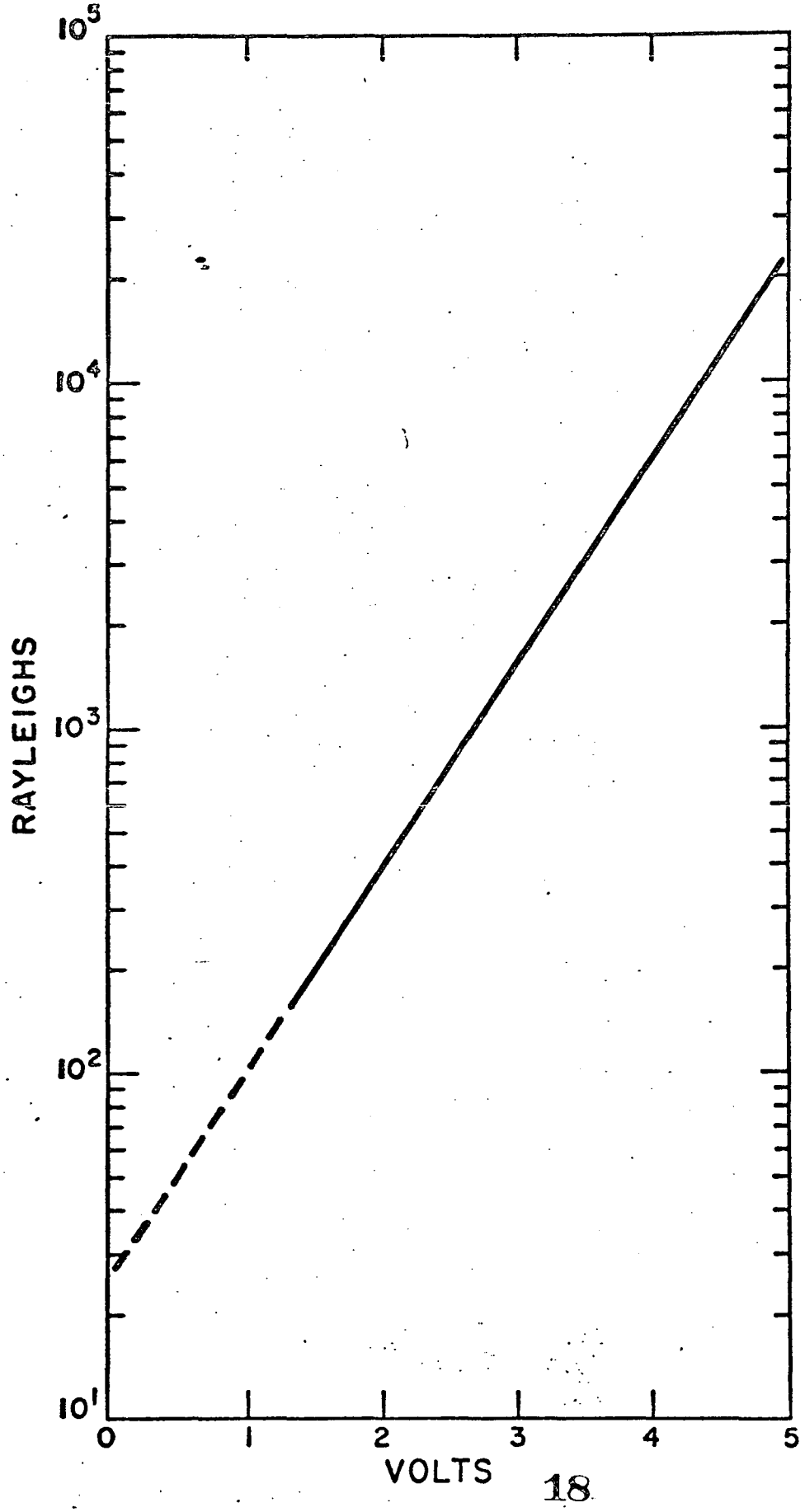
10^5
10^4
10^3
10^2
10^1
RAYLEIGHS
0
1
2
3
4
5
VOLTS

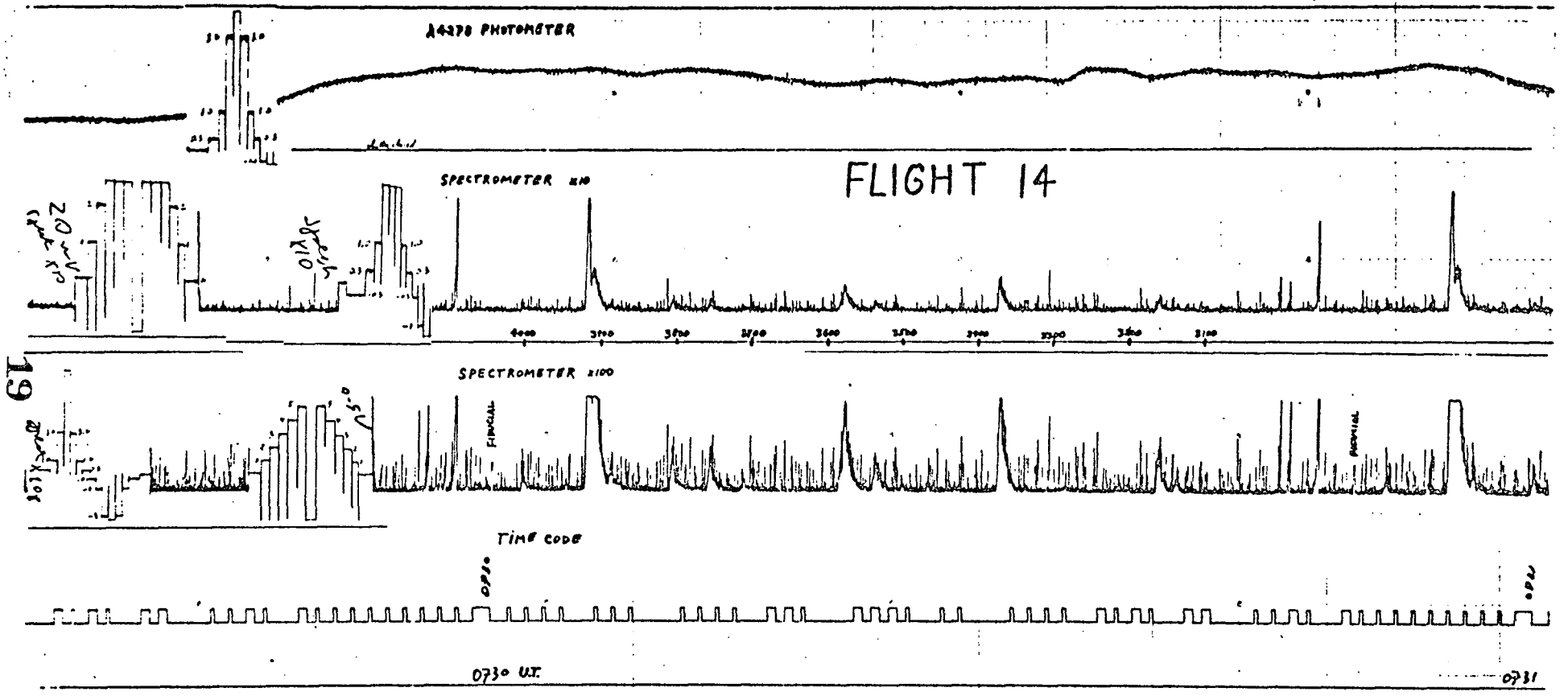
λ4278 PHOTOMETER
FLIGHT 14
SPECTROMETER x10
SPECTROMETER x100
TIME CODE
0730 U.T.
0731

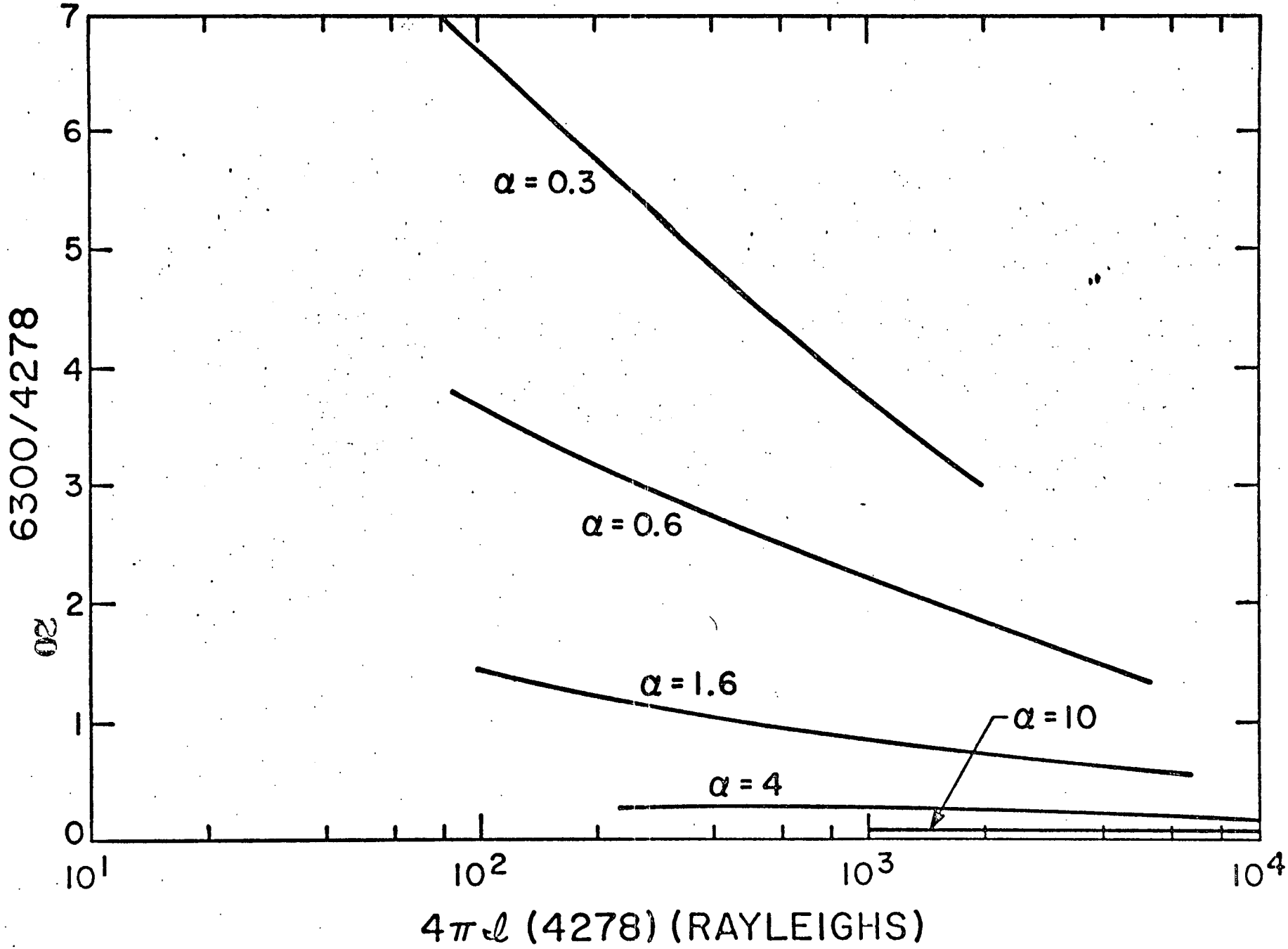
7
6
5
4
3
2
1
0
6300/4278
α = 0.3
α = 0.6
α = 1.6
α = 10
α = 4
10¹
10²
10³
10⁴
4πℓ (4278) (RAYLEIGHS)

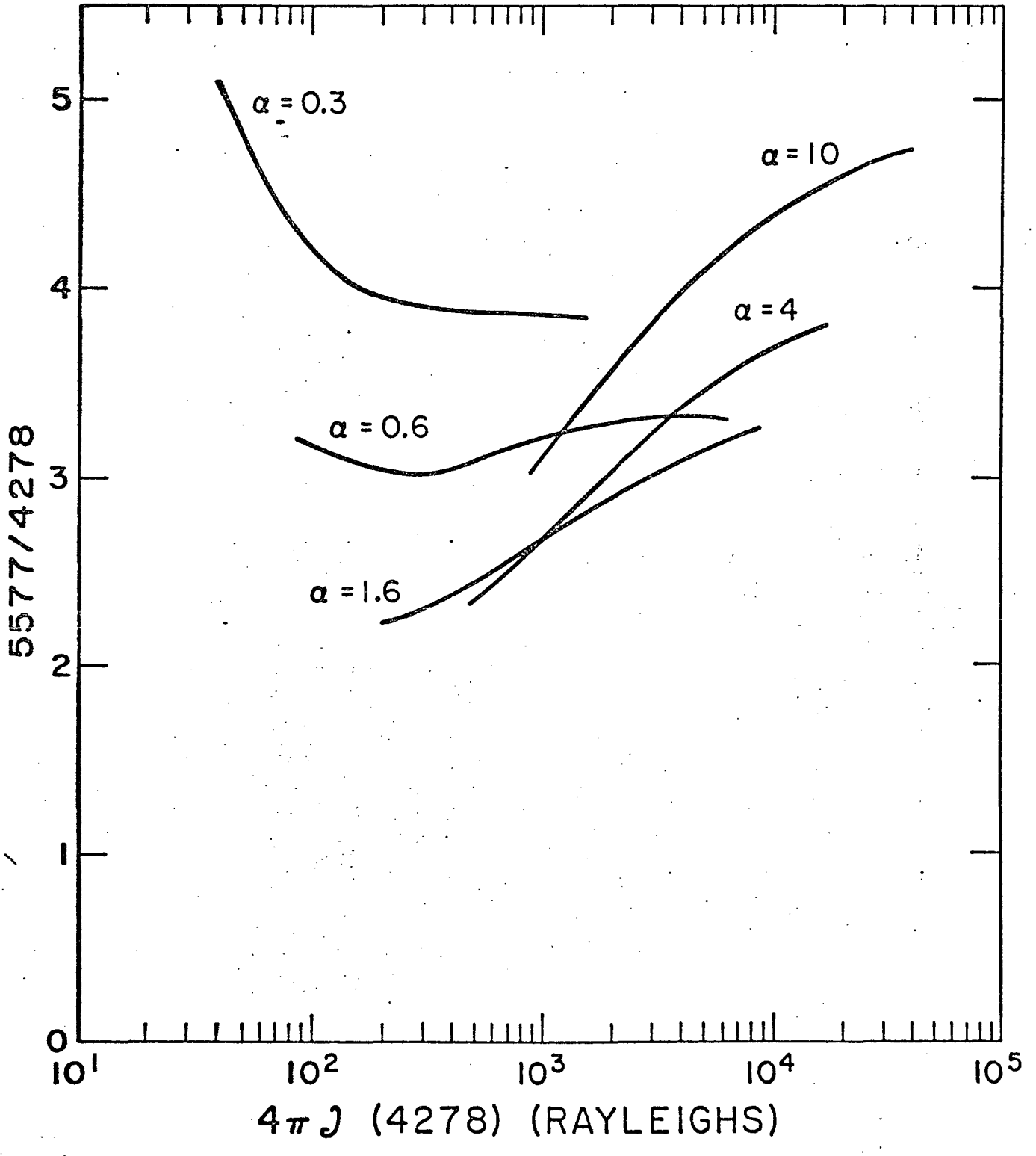
α = 0.3
α = 10
α = 4
α = 0.6
α = 1.6
5577/4278
0
1
2
3
4
5
10¹
10²
10³
10⁴
10⁵
4π J (4278) (RAYLEIGHS)

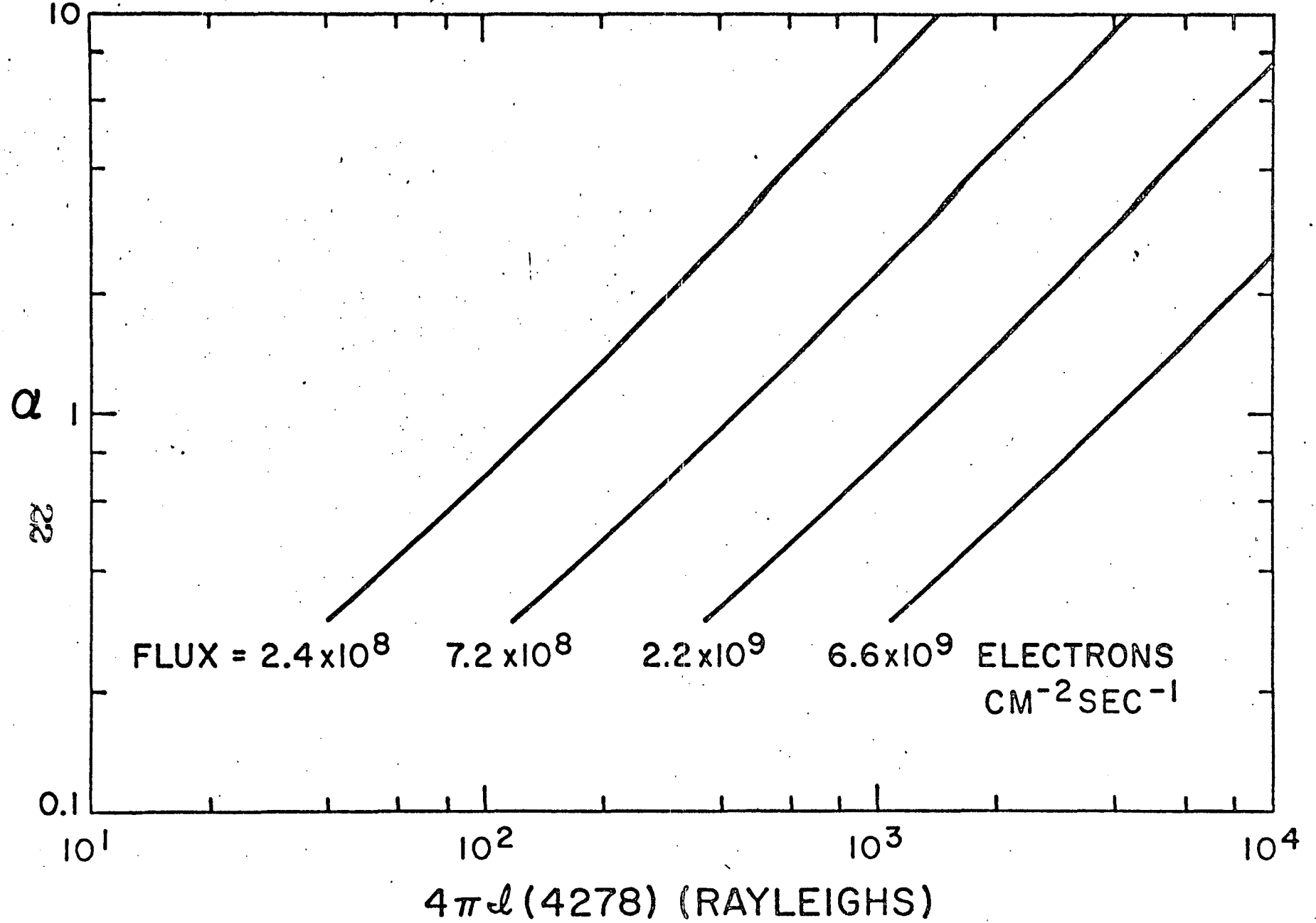
10
1
0.1
α
22
FLUX = 2.4x10^8
7.2x10^8
2.2x10^9
6.6x10^9 ELECTRONS
CM^-2 SEC^-1
10^1
10^2
10^3
10^4
4πℒ(4278) (RAYLEIGHS)

Auroral Spectrum between 1200 and 4000 Angstroms

WILLIAM E. SHARP

High Altitude Engineering Laboratory
University of Michigan, Ann Arbor, Michigan 48105

MANFRED H. REES

Laboratory for Atmospheric and Space Physics
University of Colorado, Boulder, Colorado 80302

Spectroscopic observations of an auroral event were made simultaneously by airborne and satellite-borne scanning spectrometers, in the wavelength region between 1200 and 4000 A. Photon emission rates of several vibrational bands of the N_2, 2nd positive, Vegard-Kaplan, and Lyman-Birge-Hopfield systems, the N I lines at 1200 A and 3466 A, and O I lines at 1304 A, 1356 A, and 2972 A were recorded. Model calculations of the emission rates of the observed features are found to be in reasonable agreement with the measurements. Electron impact excites the nitrogen band systems, as well as the OI 1356-A line. A spectral feature at 2150 A is tentatively identified as the (1, 0) gamma band of NO.

Simultaneous measurements of many spectral lines and bands extending over a wavelength interval from the far ultraviolet to the infrared provide a good test for models of auroral excitation. It is important that the observations be made on a single 'auroral event.' The literature abounds with unrelated measurements on auroras that probably were produced by a variety of incident electron (or proton) fluxes and energy distributions. Such unrelated observations cannot, a priori, be used to test models for excitation of the auroral spectrum, because some features are closely related through cascading or recombination processes, whereas others originate from more than one mechanism at different altitude levels, so that even ratios of spectral features are not necessarily constant from one aurora to another. The most direct procedure for testing the consistency of a model of auroral excitation is to start with a known energetic particle precipitation event and from this deduce the auroral spectrum. The larger the number of observed lines and bands available for comparison between theory and observation, the greater are the demands placed on the model. We show in this paper that, in the absence of direct particle measurements, model calculations can be used to infer the characteristics of the precipitating electron flux solely from spectral observations and to obtain a self-consistent spectroscopic description of a particular auroral event.

In spite of the simplicity of the basic concept of measuring the auroral spectrum over a wide wavelength range, the opportunities have been rare. A rocket payload flown in 1960 [*Crosswhite et al.*, 1962] obtained spectra between 1200 and 3500 A. This pioneering effort showed the presence of many vibrational bands of several systems of molecular nitrogen, 2PG, V-K, and LBH. Unfortunately, instrumental problems allowed only a marginal evaluation of absolute photon fluxes. Other rocket-borne experiments have been carried out (see *Vallance Jones* [1971] for a recent review of observations), but the wavelength range has been limited in favor of high resolution. A combination of satellite-borne instrumentation and ground-based observations provides another possibility for obtaining the required data. Such an opportunity presented itself during the 1968 NASA-Ames Auroral Airborne Expedition. Many hours were logged by the NASA CV 990 aircraft on flights in the northern auroral regions. On six occasions, the aircraft flight path intercepted the ground track of the polar orbiting satellite Ogo D passing overhead. One of the experiments on board the satellite was the University of Colorado

scanning ultraviolet spectrometer [*Barth and Mackey*, 1969]. The University of Colorado also had a scanning spectrometer aboard the aircraft. Of the six coordinations, only one occurred during an aurora of sufficient intensity to provide useful measurements. The airborne and satellite spectra, in the range 1200 to 4100 A, refer to a single auroral event, and we present the observations and analysis in this note.

EXPERIMENT

The satellite instrument is a ¼-meter Ebert-Fastie scanning spectrometer with a nominal *f*/4 focal ratio. The spectral region between 1100 and 3400 A is scanned with 20-A resolution. Two scan periods, 37.25 and 9.3 sec, are available. The shorter period was used for the coordination to be discussed. An EMR 541 G-08 photomultiplier is used to detect short wavelengths from 1100 to 1750 A, and an EMR 541 F-05 photomultiplier is used for long wavelengths of 1750 to 3400 A. The second order of the short wavelength channel is also recorded. A beam splitter at the exit slit is used to pass the long-wavelength light to the *F* tube. The instrument looked in the satellite's nadir with a field of view of 11°, a matter of importance in discussing the observed aurora.

The airborne instrument is a ½-meter Fastie-Ebert scanning spectrometer with an *f*/5 focal ratio, variable curved slits, variable wavelength interval, and adjustable scanning speed. For the coordination experiment, the wavelength interval 3000 to 4000 A was scanned in 16 sec at 7-A resolution. The peak sensitivity of the instrument with the grating and tube used is at 3500 A. The field of view of this spectrometer is 11°, and it looked in the zenith through a quartz window. The photomultiplier tube output is fed to an electrometer, thence to a 1024 channel memory storage device or directly to a strip-chart recorder.

AIRCRAFT-SATELLITE INTERCEPT

The behavior of the aurora, the aircraft, and the satellite are crucial in the interpretation of the observations. All-sky photographs obtained from the aircraft, and shown in Figure 1, reveal that a fold in an auroral band moved westward into the field of view of the airborne spectrometer (indicated by the small circles) during the coordination that occurred on February 29, 1968. Figure 2 is a time history of the brightness of the aurora in the N_2^+ 1N(0, 0) band recorded by the airborne spectrometer; an emission rate of about 7.5 kR was reached when the fold was entirely within the field of view. The fold continued moving westward out of the field of view and diminished in spatial extent but apparently not in brightness. At this time Ogo passed overhead; in the last two frames of Figure 1, the field of view at 110 km of the satellite-borne spectrometer is indicated by the large open circles.

During intercept, the satellite was at an altitude of 560 km and 0.5° in longitude west of the airplane. With an 11° field of view, an area approximately 86 km across was viewed at an altitude of 110 km, the altitude of peak energy deposition in the aurora (see below). The satellite had a speed of 6.8 km/sec and a spectral scan required 9½ sec; therefore, the satellite moved 63 km during a wavelength scan. The aircraft was at an altitude of 10 km during the intercept. The spectrometer viewed an area 20 km across at 110 km. With a 16-sec spectral scan and an aircraft speed of 550 miles/hour, the plane moved 4.5 km during a scan, a small distance compared to the satellite. The airborne spectrometer recorded the bright auroral patch in the zenith from 4h 58m 30s UT to 4h 59m 20s UT with a nearly constant emission rate of 7.5 kR, N_2^+ (λ3914). We have chosen the satellite scan around 5h 0m 40s UT as representing the best time at which the aurora was recorded from above as from below. The southern circle in frame 5h 0m 30s of Figure 1 represents the field while the 2900-A wavelength region is scanned, whereas the northward circle corresponds to the 2000-A region; in the last frame, the northern circle corresponds to the 1100-A region. Thus, though the time is not coincident, we believe that the aurora recorded on the two spectrometers is as nearly the same as circumstances permit.

OBSERVATIONAL RESULTS

Figure 3 is a composite of the auroral spectra obtained in the experiment. The spectrum from the airborne instrument in Figure 3*a* is the average of four scans taken during the time the aurora filled the field of view. Three bands are truncated by the memory storage unit be-

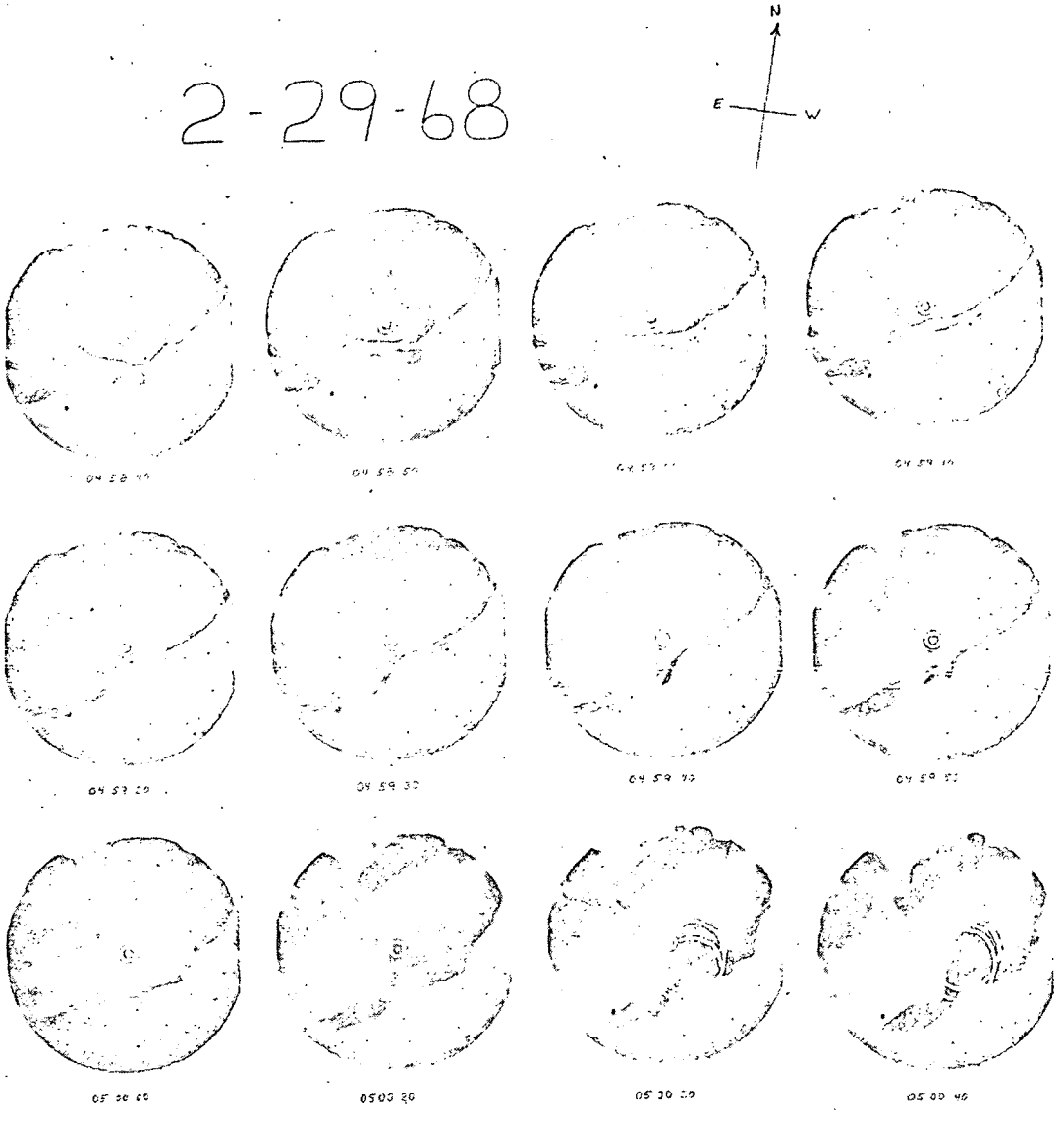

Fig. 1. All-sky-camera photographs of the aurora of February 29, 1968, used in the coordination experiment; photographs were taken from the NASA CV 990 aircraft looking in the zenith. Universal times are given. Small circles represent field of view of airborne spectrometer and large circles represent field of view of satellite spectrometer. The pictures are photographic negatives.

cause the signal from the tube exceeded the available number of counts. The direct-readout low-gain channel provided on-scale readings. The absolute response of the instrument is shown with an extinction correction applied to the low-wavelength region. The satellite data in Figure 3*b* represent a single scan; the sensitivity of this instrument is shown to first and second order.

The major spectral features originate from N_2, and a few features belong to O and N. All have been previously identified and, with the exception of the region between 1900 and 2400 A, have been confirmed. The wavelength scans

of the satellite and airborne spectrometers overlap between 3100 and 3250 A, and we note that the photon flux in the bands that lie in this interval is about the same for both instruments.

There is an emission feature at 2150 A that is usually present on bright auroral Ogo D spectra, and it appears on the coordination spectrum under study. The N_2 V-K (1, 2) band and the LBH, $\Delta v = 9$, sequence occur in this wavelength region, but the predicted intensity of these two features relative to other bands in their systems is far too small to account for the observed emission rate. We identify the spectral feature at 2150 A with the 1,0 band of the NO γ system. *Duysinx and Monfils* [1971] have reported observations of NO γ bands in UV auroral spectra.

There are many noise spikes that appear on the satellite spectrum. They can be identified by a characteristic sharp rise time, and they frequently occur on top of real spectral features. Indeed, there appears to be a connection between the magnitude of the signal and the noise when the latter is present, requiring special care in the analysis.

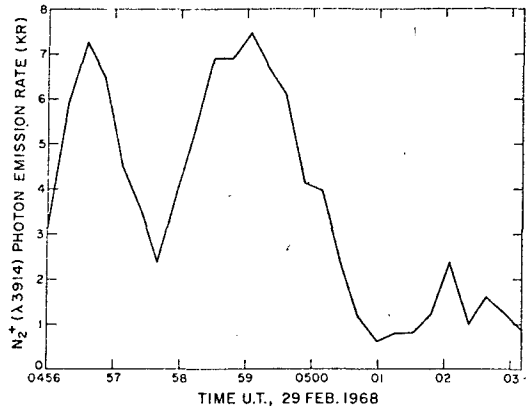

Fig. 2. Time history of auroral brightness as recorded by the airborne spectrometer in the N_2^+ 1N (0, 0) radiation.

ANALYSIS

Synthetic spectra for the N_2 V-K and LBH band systems were constructed using the results of *Shemansky* [1969*a*, *b*]. The 0,5 band was used to normalize the synthetic to the observed V-K system spectrum, and the 1,1 and 2,1 vibrational bands were used for the LBH system. These choices were governed by considerations of signal strength and signal-to-noise ratio. The dotted lines in Figure 3*b* are the normalized synthetic spectra of the two band systems. Over the entire wavelength region, the amplitude of the synthetic spectrum is always less than the observed one, which includes additional spectral features and noise. Our procedure does not overestimate, but may underestimate the photon flux of the LBH bands. Band system emission rates were evaluated from the area under the synthetic spectrum. The (0, 0) vibrational band was used to infer the intensity of the N_2 2PG system by

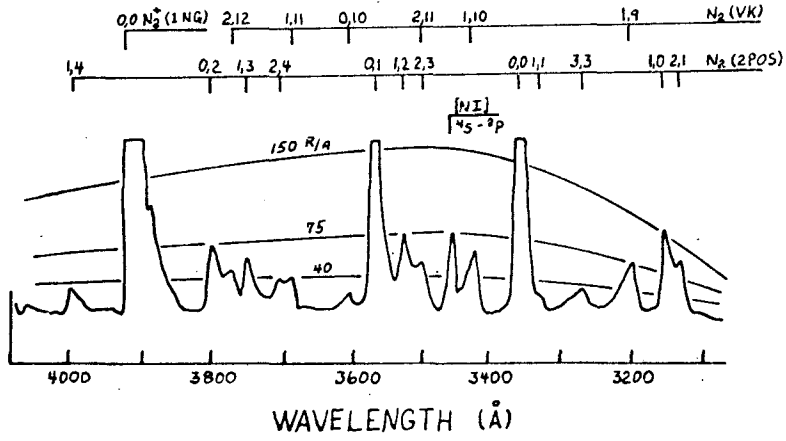

Fig. 3*a*. Auroral spectrum in the near ultraviolet recorded by the airborne spectrometer. This spectrum is a composite of four 16-sec scans at a 7-A spectral resolution. The instrument sensitivity is shown, along with identified spectral features.

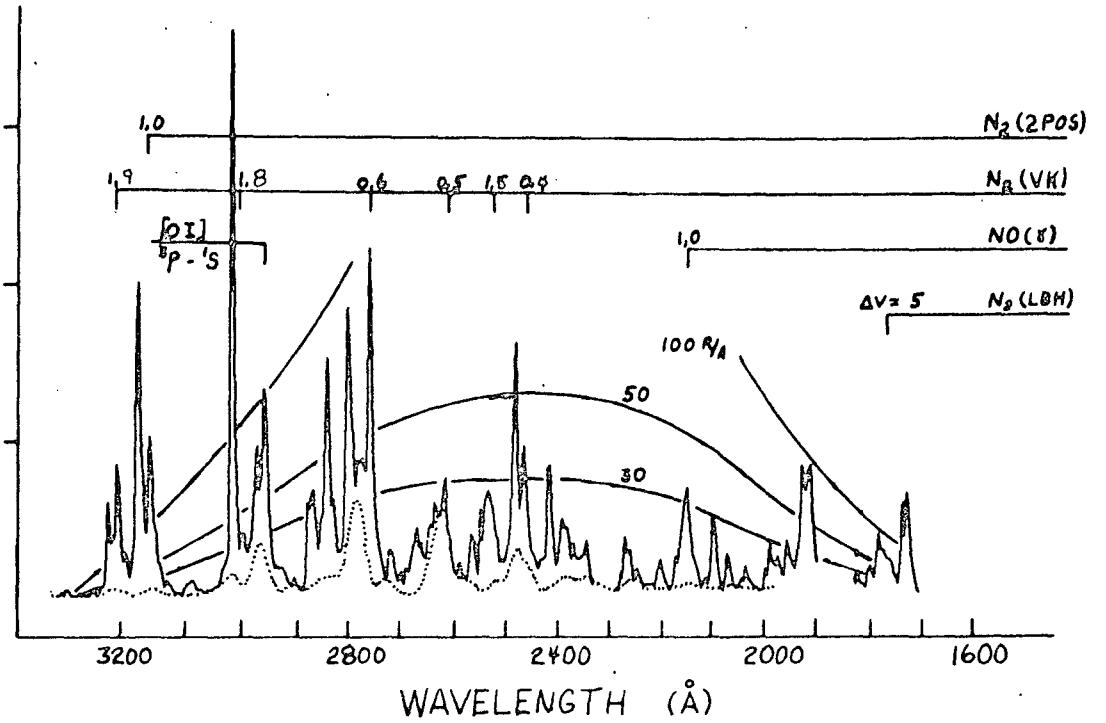

Fig. 3*b*. Auroral spectrum in the far ultraviolet recorded by the satellite spectrometer. The spectrum above was recorded by a *F*-type photomultiplier tube and shows identified spectral features. A *G*-type PM tube recorded the spectrum on the opposite page. Synthetic spectra are shown by dotted curves.

assuming that the relative population of the vibrational levels is due to direct electron impact. Photon fluxes of the observed molecular and atomic emission features are listed in Table 1. These observed fluxes are lower limits, since the satellite spectrometer field of view was not completely filled.

An energetic particle detector was one of the experiments on board the Ogo D satellite; however, the data format that provided the 9½ sec UV spectrometer scan excluded several of the other experiments, including the particle detectors. We have therefore used a method for deducing the incident particle flux and energy spectrum that requires as known inputs only the photon flux in one of the N_2^+1N bands and the ratio of emission rates of the red oxygen line and a first negative band, O I (λ6300)/N_2^+ (λ4278). The N_2^+1N excitation is directly proportional to the ionization rate, but the atomic oxygen lines are excited by several mechanisms, principally electron impact and dissociative recombination, each with its own altitude profile. In addition, the O(^{1}D) level is collisionally de-excited at low altitudes, rather than radiatively. Thus, column emission rates of the various spectral features depend on the altitude profile and magnitude of the energy deposition rate, i.e., the spectral distribution and magnitude of the precipitating electron flux. M. H. Rees, R. H. Eather, and S. B. Mende (unpublished data, 1971) have computed the photon emission rates of N_2^+ (λ4278), O I (λ6300), and O I (λ5577) over a range of electron fluxes and spectral distributions that should include almost all situations encountered in auroral measurements. They find that if the electron spectrum is not too hard the ratio λ6300/λ4278 as a function of λ4278 photon emission rate becomes a sensitive indicator of the primary electron energy spectrum.

We did not measure the O I (λ6300) and O I (λ5577) lines with the scanning spectrometer; however, R. H. Eather had a 4-channel tilting filter photometer on the aircraft and has kindly provided his observations during the

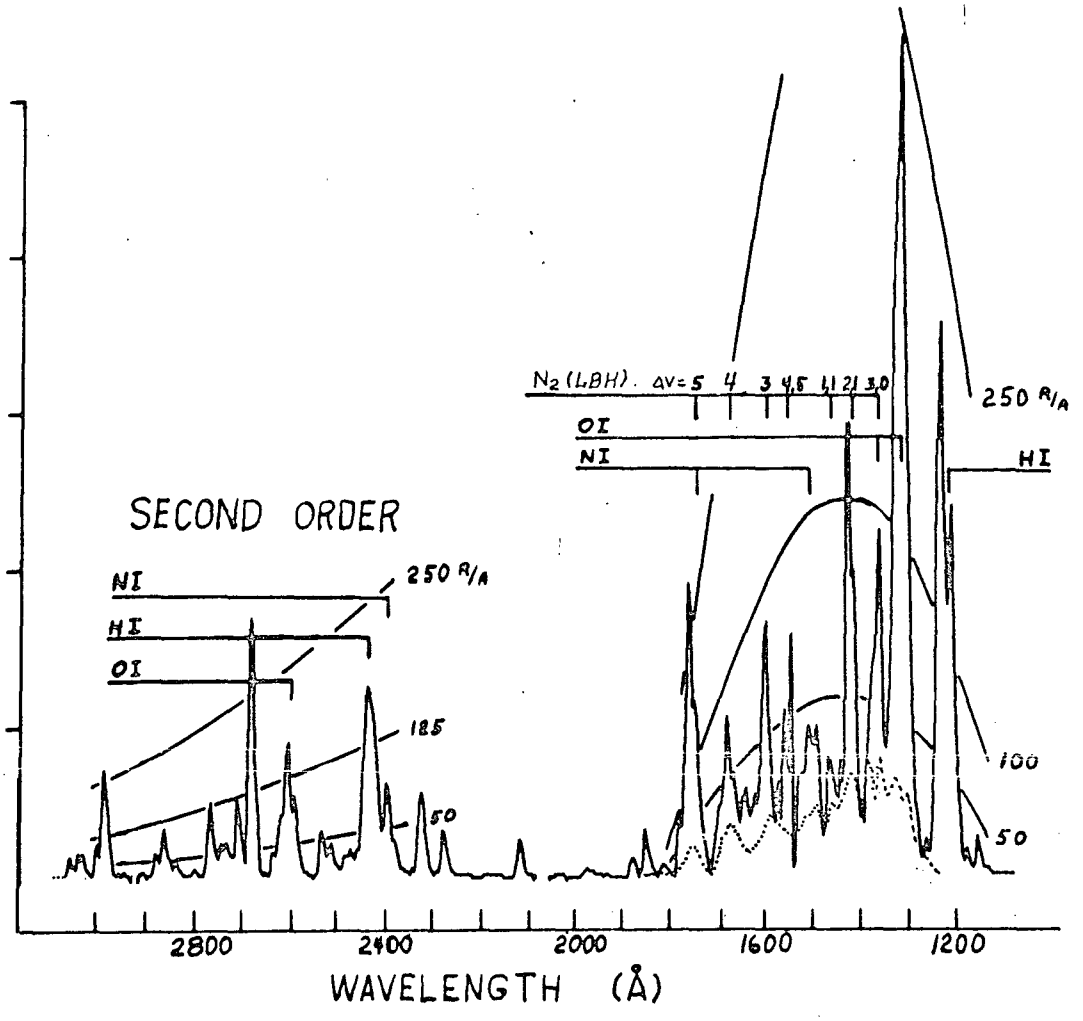

Fig. 3*b* (continued)

coordination experiment. He obtained an emission rate of 1.15 kR for the O I (λ6300) radiation. The λ4278 photon emission rates from Eather's photometer are about one-third of our λ3914 measurements, in agreement with the predicted ratio of the two band intensities. Our computed λ5577 emission rates agree very well with Eather's observations. Eather notes that the hydrogen Balmer beta radiation was small during this period, and proton bombardment makes a negligible contribution to the ionization and excitation of the auroral spectrum.

We find that a flux of 1.75×10^0 electrons cm^{-2} sec^{-1} having a power-exponential spectrum with characteristic energy of 2.3 kev satisfies the aurora under study, i.e., it produces an emission rate of 7.5 kR of λ3914 and a ratio λ6300/λ4278 of 0.46. The altitude of maximum energy deposition is 112 km, and the total rate of energy deposition is 12.9 ergs cm^{-2} sec^{-1}.

The spectral features for which we predict emission rates are excited primarily by low-energy electrons, and we next compute the differential flux of secondary electrons. The procedure is given by *Rees et al.* [1969], but we now use production rates derived from laboratory experiments of *Opal et al.* [1971] in place of the theoretical values derived from the Bethe approximation. We have also included a new expression for the electron energy loss given by *Schunk and Hays* [1971]. These improvements, and the use of an energy grid tighter than the

TABLE 1. Computed and Observed Emission Rates in Kilorayleighs

Band System or Line	Computed Photon Emission Rate	Measured Photon Emission Rate		
		Aircraft	Satellite	Channel
N_2^+ (λ3914)	7.5	7.5		
N_2 2PG	17.3	15		
N_2 V-K $v' = 0$	4.6		4.0	F
$v' = 1$	3.0	4.5	3.5	
N_2 LBH	14.2–20		11	G
O I (λ1356)	0.9–1.0		1.0	G
(λ2972)	0.31		0.4	F
(λ1300)			5.1	G
N I (λ1200)			1.2	G
(λ3466)		0.6		
H (λ1216)			4.9	G
NO γ(1, 0)			0.9	F

one used by *Rees et al.* [1969], produce a spectrum that no longer has a sharp minimum at 15 ev. The differential electron flux is given in Table 2 at a few values of altitude and energy.

The differential electron flux $\varphi(E, z)$ and the excitation cross section $\sigma(E)$ are needed to compute the production rates of excited states,

$$\eta(z) = N(X) \int_{E_{th}}^{\infty} \varphi(E, z)\sigma(E)\, dE \quad \text{cm}^{-3}\,\text{sec}^{-1}$$

where $N(X)$ is the number density of atomic or molecular species X, and E_{th} is the excitation threshold. We have computed the excitation rate of the $A^3\Sigma$, $B^3\Pi$, and $C^3\Pi$ states of N_2 using cross sections (Cartwright, private communication) similar to those of *Brinkmann and Trajmar* [1970], and for the $N_2a^1\Pi$ state we have used cross sections given by *Ajello* [1970] and by *Holland* [1969]. For excitation of the O I (λ1356), line we have used the total cross sections of *Zipf et al.* [1971]. The population of the ground configuration O(^{1}S) level is computed as described by M. H. Rees, R. H. Eather, and S. B. Mende (unpublished data, 1971) and we assume that the radiation in the λ2972 line accounts for 1/17 of the population rate of the excited state.

To facilitate comparison with observations, the excitation rates of the $v' = 0$ and $v' = 1$ vibrational levels of the $A^3\Sigma$ state are computed separately using the method given by *Sharp* [1971, equation 11]. The metastable $A^3\Sigma$ state has a radiative lifetime of about 2 sec, and is collisionally de-excited at low altitude; we have adopted the quenching rates for the $v' = 0$ and $v' = 1$ levels given by *Sharp* [1971].

The atmosphere is optically thick in the 1356 A line of atomic oxygen and in the short-wavelength LBH bands below about 120 km so that a detector viewing from above only sees the column emission rate down to about this altitude. Predicted column emission rates are obtained by integrating the volume emission rates $\eta(z)$ over the appropriate altitude interval and including quenching where required. The predicted brightness of spectral features, based solely on a 7.5-kR photon emission rate in λ3914 and the theoretical development outlined above, are given in Table 1, together with the observations.

We have identified the feature at 2150 A with the gamma band system of NO, and wish to speculate briefly about possible excitation sources. Two possibilities are electron impact on ambient NO and the quenching reaction with $N_2(A^3\Sigma)$. These two sources imply that the intensity of the 1,0 gamma band is

$$I_{1,0}{}^{\gamma} = \omega_{1,0}\left\{[N_2(A)]kf_c + \int_E \sigma_1\varphi(E)\, dE\right\}[NO]$$

where $N_2(A)$ is the concentration of $v' = 0$ of that state, k is the reaction rate coefficient, σ_1 is the cross section for electron impact excitation of the level, $\omega_{1,0}$ is the branching ratio, and f_c is the fractional population of the $v' = 1$ level of the gamma system when chemically excited. We use $k = 8 \times 10^{-11}$ cm^3 sec^{-1} [*Meyer et al.*, 1971], $f_c = 0.3$ [*Callear and Wood*, 1971],

TABLE 2. Differential Electron Flux†

Energy, ev	Altitude, km					
	105	110	115	120	130	150
4.0	6.26(+8)*	2.14(+9)	3.61(+9)	4.21(+9)	5.29(+9)	5.27(+9)
4.5	7.99(+8)	2.58(+9)	4.15(+9)	4.66(+9)	5.60(+9)	5.38(+9)
5.0	8.29(+8)	2.63(+9)	4.16(+9)	4.63(+9)	5.49(+9)	5.22(+9)
5.5	5.51(+8)	1.86(+9)	3.12(+9)	3.62(+9)	4.54(+9)	4.55(+9)
6.0	3.32(+8)	1.20(+9)	2.17(+9)	2.68(+9)	3.64(+9)	3.94(+9)
6.5	1.52(+8)	5.83(+8)	1.11(+9)	1.46(+9)	2.18(+9)	2.69(+9)
7.0	8.98(+7)	3.49(+8)	6.78(+8)	9.01(+8)	1.40(+9)	1.85(+9)
7.5	5.07(+7)	1.99(+8)	3.90(+8)	5.24(+8)	8.37(+8)	1.16(+9)
8.0	2.29(+7)	9.02(+7)	1.78(+8)	2.42(+8)	3.94(+8)	5.71(+8)
8.5	1.31(+7)	5.18(+7)	1.03(+8)	1.42(+8)	2.35(+8)	3.49(+8)
9.0	8.76(+6)	3.49(+7)	6.98(+7)	9.60(+7)	1.60(+8)	2.41(+8)
9.5	7.18(+6)	2.86(+7)	5.74(+7)	7.92(+7)	1.32(+8)	2.00(+8)
10.0	6.07(+6)	2.41(+7)	4.82(+7)	6.61(+7)	1.10(+8)	1.63(+8)
10.5	5.44(+6)	2.15(+7)	4.27(+7)	5.81(+7)	9.52(+7)	1.39(+8)
11.0	4.93(+6)	1.94(+7)	3.83(+7)	5.18(+7)	8.39(+7)	1.20(+8)
11.5	5.13(+6)	2.00(+7)	3.92(+7)	5.26(+7)	8.39(+7)	1.17(+8)
12.0	5.32(+6)	2.06(+7)	4.00(+7)	5.32(+7)	8.32(+7)	1.12(+8)
12.5	4.62(+6)	1.78(+7)	3.44(+7)	4.55(+7)	7.05(+7)	9.43(+7)
13.0	4.02(+6)	1.55(+7)	2.97(+7)	3.90(+7)	6.02(+7)	7.99(+7)
13.5	3.51(+6)	1.35(+7)	2.58(+7)	3.39(+7)	5.21(+7)	6.90(+7)
14.0	3.09(+6)	1.18(+7)	2.27(+7)	2.97(+7)	4.55(+7)	6.00(+7)
15.0	2.96(+6)	1.13(+7)	2.16(+7)	2.82(+7)	4.31(+7)	5.66(+7)
16.0	2.66(+6)	1.02(+7)	1.95(+7)	2.55(+7)	3.91(+7)	5.14(+7)
17.0	2.31(+6)	8.90(+6)	1.71(+7)	2.25(+7)	3.49(+7)	4.66(+7)
18.0	1.99(+6)	7.68(+6)	1.49(+7)	1.97(+7)	3.07(+7)	4.17(+7)
19.0	1.72(+6)	6.66(+6)	1.30(+7)	1.72(+7)	2.71(+7)	3.73(+7)
20.0	1.50(+6)	5.83(+6)	1.14(+7)	1.52(+7)	2.41(+7)	3.34(+7)
25.0	7.81(+5)	3.05(+6)	5.98(+6)	8.04(+6)	1.29(+7)	1.82(+7)
30.0	4.73(+5)	1.85(+6)	3.64(+6)	4.90(+6)	7.89(+6)	1.13(+7)
35.0	3.23(+5)	1.27(+6)	2.49(+6)	3.35(+6)	5.38(+6)	7.68(+6)
40.0	2.43(+5)	9.53(+5)	1.87(+6)	2.52(+6)	4.05(+6)	5.77(+6)
50.0	1.48(+5)	5.78(+5)	1.14(+6)	1.53(+6)	2.45(+6)	3.48(+6)
70.0	7.69(+4)	3.01(+5)	5.89(+5)	7.90(+5)	1.26(+6)	1.78(+6)
100	3.93(+4)	1.54(+5)	3.00(+5)	4.02(+5)	6.40(+5)	8.96(+5)
200	2.32(+3)	9.03(+3)	1.76(+4)	2.36(+4)	3.74(+4)	5.20(+4)

* $6.26(+8) \equiv 6.26 \times 10^8$.
† el cm^2 sec^{-1} ev^{-1}.

$N_2(A) = 2 \times 10^9$ cm^{-3} at 110 km, according to our calculations, and $\sigma_{1,0} \approx 10^{-18}$ cm^2 (Ajello, private communication). If the electron-impact cross section peaks at an energy twice to three times threshold, $\varphi \approx 3 \times 10^7$ cm^{-2} sec^{-1} ev^{-1}, according to Table 2. With these parameters the first term in the brackets dominates by more than an order of magnitude. Thus we find that $I_{1,0}^{\gamma} \approx 1.2 \times 10^{-8}$ [NO] at about 110 km. Assuming that the scale height of the NO density and emission are the same and that half the emission originates from below 110 km, our emission rate implies a column density of [NO] above 110 km of 7.5×10^{16} cm^{-2}. Such a very high density has been reported by *Zipf et al.* [1970].

DISCUSSION

Previous efforts to compare observed with model UV auroral spectra [e.g., *Barth*, 1968] have shown large discrepancies. We attribute the improved agreement achieved in this experiment principally to the fact that all the observations are made as nearly as possible on the same 'auroral event.'

Nevertheless, we can find many possible sources of uncertainty. On the theoretical side, we have arbitrarily assumed a power-exponen-

tial electron energy distribution. Most electron precipitation events can be so represented [e.g., *Belon et al.*, 1966; *Frank and Ackerson*, 1971] and the details of the primary spectrum do not strongly influence the low-energy secondary spectrum that dominates the excitation of the spectral features discussed here. There are and probably always will be uncertainties about the absolute values of excitation cross sections and reaction rates that are used abundantly in the theoretical computations; excitation processes that might contribute to emission may have been overlooked.

We have not attempted to predict the photon emission rates of the N I lines, because we do not know which processes contribute to the excitation, e.g., dissociative ionization excitation, dissociative excitation, dissociative recombination, or electron impact. In such cases a profile of experimental volume emission rate versus altitude is required to make any progress on the interpretation.

No theoretical predictions are given for the O I (λ1300) triplet. This resonance radiation undoubtedly undergoes multiple scattering, and we have not made this calculation.

On the experimental side, we have already noted the large difference in fields of view between the satellite and the airborne spectrometers shown in Figure 1. In addition, the aurora did not completely fill the field of view of the satellite spectrometer and included slightly different regions of the aurora during a spectral scan. It is our personal opinion that the airborne spectrometer calibration is more reliable than the satellite instrument, but we are not able to provide error bars for either one.

The observed hydrogen Lyman-α line has an emission rate during the auroral event that is no different from the ordinary nighttime scattered radiation, and no auroral enhancement is indicated, in agreement with the H_β measurements of Eather (private communication) made from the aircraft.

Acknowledgments. L. Haughney and M. Bader of the Airborne Science Office, NASA-Ames Research Center, and the pilots and crew of the CV 990 are responsible for the success of the airborne expedition. S. I. Akasofu kindly gave use the all-sky-camera photographs, R. H. Eather provided us with some of his photometric data, and C. A. Barth supplied the Ogo D spectrometer data.

Financial support was provided by NASA grant NGR-06-003-110.

* * *

The Editor thanks A. Vallance Jones and another referee for their assistance in evaluating this paper.

REFERENCES

Ajello, J. M., Emission cross sections of N_2 in the vacuum ultraviolet by electron impact, *J. Chem. Phys., 53,* 1156, 1970.

Barth, C. A., The spectrum of the ultraviolet aurora, *Ann. Geophys., 24,* 1, 1968.

Barth, C. A., and E. F. Mackey, Ogo 4 ultraviolet airglow spectrometers, *IEEE Trans. Geosci. Electron., 7,* 114, 1969.

Belon, A. E., G. J. Romick, and M. H. Rees, The energy spectrum of primary auroral electrons determined from auroral luminosity profiles, *Planet. Space Sci., 14,* 597, 1966.

Brinkmann, R. T., and S. Trajmar, Electron impact excitation of N_2, *Ann. Geophys., 26,* 201, 1970.

Callear, A. B., and P. M. Wood, Rates of energy transfer from N_2 ($A^3\Sigma_u^+$) to various molecules, *Trans. Faraday Soc., 67,* 272, 1971.

Crosswhite, H. M., E. C. Zipf, Jr., and W. G. Fastie, Far ultraviolet auroral spectra, *J. Opt. Soc. Amer., 52,* 643, 1962.

Duysinx, R., and A. Monfils, Auroral spectra recorded between 2000 A and 3000 A with a fast scanning spectrometer, paper presented at the Fifteenth IUGG General Assembly, Moscow, 1971.

Frank, L. A., and K. L. Ackerson, Observations of charged particle precipitation into the auroral zone, *J. Geophys. Res., 76,* 3612, 1971.

Holland, R. F., Excitation of nitrogen by electrons: The Lyman-Birge-Hopfield system of N_2, *J. Chem. Phys., 51,* 3940, 1969.

Meyer, J. A., D. W. Setser, and W. G. Clark, Rate constants for quenching of $N_2(A^3\Sigma_u^+)$ in active nitrogen, *J. Chem. Phys.*, in press, 1971.

Opal, C. B., W. K. Peterson, and E. C. Beaty, Measurements of secondary electron spectra produced by electron impact ionization of a number of simple gases, *J. Chem. Phys., 55,* 4100, 1971.

Rees, M. H., A. I. Stewart, and J. C. G. Walker, Secondary electrons in aurora, *Planet. Space Sci., 17,* 1997, 1969.

Schunk, R. W., and P. B. Hays, Photoelectron energy losses to thermal electrons, *Planet. Space Sci., 19,* 113, 1971.

Sharp, W. E., Rocket-borne spectroscopic measurements in the ultraviolet aurora: Nitrogen Vegard-Kaplan bands, *J. Geophys. Res., 76,* 987, 1971.

Shemansky, D. E., The N_2 Vegard-Kaplan system in absorption, *J. Chem. Phys., 51,* 689, 1969*a*.

Shemansky, D. E., Transition probabilities and collision broadening cross section of the N_2

Lyman-Birge-Hopfield system, *J. Chem. Phys., 51,* 5487, 1969*b*.
Vallance Jones, A., Auroral spectroscopy, *Space Sci. Rev., 11,* 776, 1971.
Zipf, E. C., W. L. Borst, and T. M. Donahue, A mass spectrometer observation of NO in an auroral arc, *J. Geophys. Res., 75,* 6371, 1970.
Zipf, E. C., E. J. Stone, M. J. Mumma, W. L. Wells, and W. L. Borst, Excitation of the OI(^{3}S) states by electron impact on O and O_2 in the aurora, dayglow and EEUV, *Eos Trans. AGU, 52,* 308, 1971.

(Received November 4, 1971;
accepted December 21, 1971.)

JOURNAL OF GEOPHYSICAL RESEARCH, SPACE PHYSICS VOL. 75, NO. 25, SEPTEMBER 1, 1970

Latitude Distribution of Night Airglow

W. E. SHARP AND M. H. REES

Laboratory for Atmospheric and Space Physics
University of Colorado, Boulder 80302

This note reports measurements of nightglow radiations obtained over a wide range of geographic latitude. A scanning spectrometer was one of several instruments aboard a Convair 990 aircraft during the NASA auroral airborne expedition of 1968. Four flights at low and middle latitudes and three polar cap flights were made that for the largest portion were outside the auroral oval (see Figure 1 of *Dick et al.* [1970]). The polar cap flights occurred during magnetically quiet conditions. During these airglow flights the Herzberg I system of O_2 in the near ultraviolet and the [O I] 5577-A line were recorded.

The half-meter Ebert-Fastie [*Fastie*, 1952] spectrometer has a focal ratio of $f/5.0$, variable slits, and maximum sensitivity in the near ultraviolet with the photomultiplier tube employed. A 1000-A wavelength interval was scanned in 32 sec at a spectral resolution of 16 A. The signal was fed to an electrometer, hence to a 1024 channel memory storage device. The system was absolutely calibrated in the laboratory to a precision of $\pm 30\%$. For most of the data presented here, the spectrometer was pointed in the zenith.

The procedure for data acquisition consisted of storing approximately 10 to 20 scans of the Herzberg I system in the memory and reading the sum out onto a chart recorder. The memory was cleared, and 3 to 6 scans of the 5577-A line were summed and read out. This sequence was followed for all airglow flights. The data points for 5577 A were averaged every 5° of invariant latitude south of 60°, and every $2\frac{1}{2}$° north of 72.5°. The data points for the Herzberg bands were averaged every $2\frac{1}{2}$° for all latitudes. The (2, 6) and (4, 7) bands of the Herzberg I system (which overlap in the wavelength interval 3620–3680 A) were used in the analysis. Any auroral contamination in this spectral region would be very weak. A sample airglow spectrum in the near ultraviolet recorded at a zenith angle of 75° is shown in Figure 1.

The near ultraviolet spectral region included the (0, 0) band of N_2^+(1N) at 3914 A. Presence of this radiation was used as an indication of auroral contamination, and data were not used in computing the averages.

Zenith emission rates were corrected for extinction and scattering by using the tables given by *Ashburn* [1954] and absorption coefficients from *Allen* [1955]. The corrections are small at the altitude of the airplane (~10 km), which in most cases was at or just below the tropopause. The observed emission rates were multiplied by the appropriate factors, 1.13 at 3640 A and 1.05 at 5577 A.

Figure 2 presents the true emission rate as a function of invariant latitude. Invariant latitude is used because it best identifies the auroral oval. The 5577-A emission rates between 60° and 72.5° are omitted because of auroral contamination or lack of measurement. The 5577-A intensities reported here are about the same as those reported by *Eather* [1969] and *Dick et al.* [1970] but are about 50% less than the averages reported by *Davis and Smith* [1965] in a latitude survey in 1962 using shipborne photometers. The latter investigators report greater variability with latitude as compared with our observations. From Figure 2 we conclude that, on the average, the 5577-A and Herzberg I emissions are constant with latitude. Figure 3 shows individual 5577-A data points as a function of local time. There is no discernible trend in the data, collectively or for individual nights. The nature of the experiment precluded reliable separation between temporal and spatial effects. *Barbier* [1955]

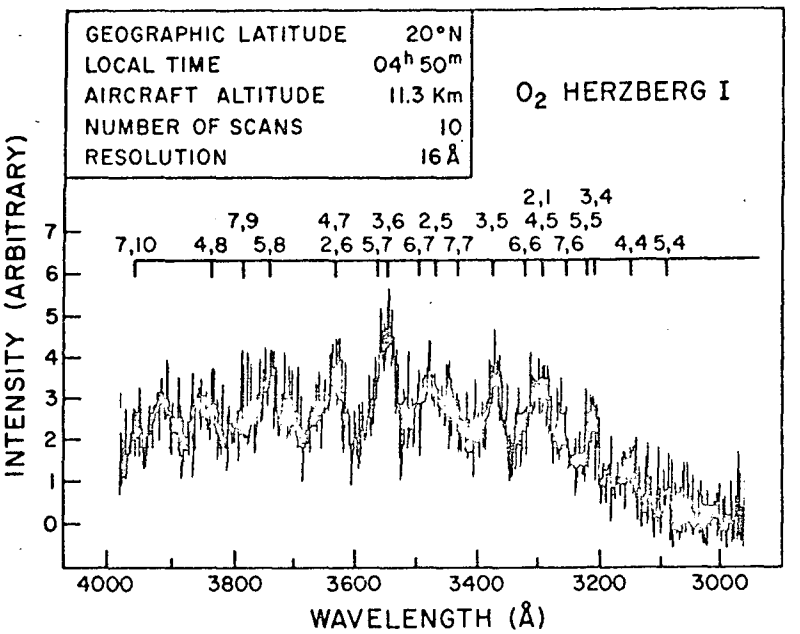

Fig. 1. The ultraviolet night airglow spectrum. Vibrational bands of the Herzberg I emissions are indicated.

found a linear relationship between the Herzberg I and [O I] 5577 emissions at a geographically fixed station.

Degen [1969] has constructed synthetic spectra of the Herzberg I system that yield relative intensities of the various vibrational bands. On the basis of this work, the sum of the intensities of the two measured vibrational bands amounts to 2% of the total emission rate in the band system. An average emission rate of about 1.5 kR is therefore obtained for the Herzberg I system in the nightglow.

The $O_2(A^3 \sum_u^+)$ state is probably produced by the three-body association of O atoms [cf. *Chamberlain*, 1961] in which any species may act as the third body.

$$O + O + M \rightarrow O_2 + M$$

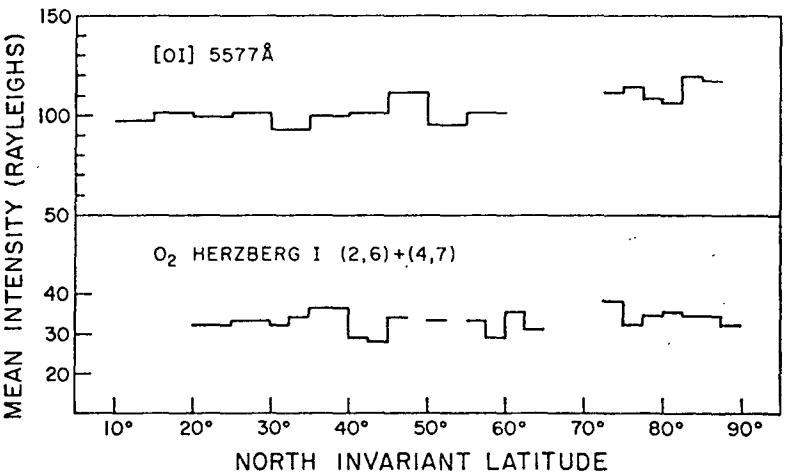

Fig. 2. The average nightglow emission rate of [O I] 5577 A and Herzberg I (2, 6) and (4, 7) as a function of invariant latitude at whatever local time observations were made.

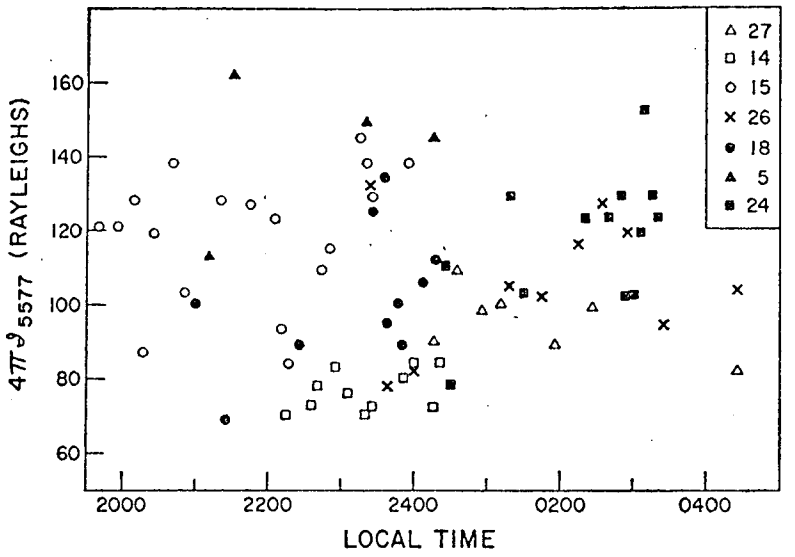

Fig. 3. The emission rate of 5577 A as a function of local time measured on each flight. Different symbols refer to the flight numbers.

The rate coefficient for this reaction (with unspecified products) is about 3×10^{-33} cm^6 sec^{-1} [*Campbell and Thrush*, 1967; *Morgan and Schiff*, 1963]. The altitude profile of the Herzberg bands peaks at 95 km and has a width of about 12 km at half-intensity [*Packer*, 1961; *Reed*, 1968]. If the atomic oxygen concentration is assumed to be 3.4×10^{11} cm^{-3} and the total particle concentration to be 2.5×10^{13} cm^{-3}, the recombination rate in the altitude interval from which the Herzberg bands originate is 1.0×10^{10} cm^{-2} sec^{-1}. Since quenching occurs below 95 km [*Barth*, 1964], comparison with the observed emission rate of the Herzberg bands of 1.5×10^9 photons cm^{-2} sec^{-1} gives a lower limit of 0.15 for the fraction of recombinations that produces the $A^3 \sum_u^+$ state of O_2.

Acknowledgments. We would like to thank the managers of the expedition, Mr. L. Haughney and Dr. M. Bader of the Airborne Sciences Office, NASA-Ames Research Center, and the pilots and crew of the Convair 990 for the success of the expedition.

This work was done while one of us (W.E.S.) held a NASA Predoctoral Traineeship. This experiment was supported by NASA, contract NGR 06-003-077.

References

Allen, C. W., *Astrophysical Quantities*, Athlone, London, 1955.

Ashburn, E. V., The effect of Rayleigh scattering and ground reflection upon the determination of the height of the night airglow, *J. Atmos. Terr. Phys.*, *5*, 83, 1954.

Barbier, D., Resultats preliminaires d'une photometrie en huit couleurs de la lumiere du ciel nocturne, in *The Airglow and the Aurorae*, edited by E. B. Armstrong and A. Dalgarno, Pergamon, London, 1955.

Barth, C. A., Three-body reactions, *Ann. Geophys.*, *20*, 182, 1964.

Campbell, I. M., and B. A. Thrush, The association of oxygen atoms and their combination with nitrogen atoms, *Proc. Roy. Soc. London, A, 296*, 22, 1967.

Chamberlain, J. W., *Physics of the Aurora and Airglow*, Academic, New York, 1961.

Davis, T. N., and L. L. Smith, Latitudinal and seasonal variations in the night airglow, *J. Geophys. Res.*, *70*, 1127, 1965.

Degen, V., Vibrational populations of O_2 ($A^3\sum_u^+$) and synthetic spectra of the Herzberg bands in the night airglow, *J. Geophys. Res.*, *74*, 5145, 1969.

Dick, K. A., G. G. Sivjee, and H. M. Crosswhite, Aircraft measurements of OII, O I, O_3, and H-alpha airglow intensities, *Planet. Space Sci.*, *18*, in press, 1970.

Eather, R. H., Latitudinal distribution of auroral and airglow emissions: The 'soft' auroral zone, *J. Geophys. Res.*, *74*, 153, 1969.

Fastie, W. G., A small plane grating monochromator, *J. Opt. Soc. Amer.*, *42*, 641, 1952.

Morgan, J. E., and H. I. Schiff, Recombination of oxygen atoms in the presence of inert gases, *J. Chem. Phys.*, *38*, 1495, 1963.

Packer, D. M., Altitudes of the night airglow radiations, *Ann. Geophys.*, *17*, 67, 1961.

Reed, E. I., A night measurement of mesospheric ozone by observations of ultraviolet airglow, *J. Geophys. Res.*, *73*, 2951, 1968.

(Received June 9, 1970.)
Communicated by D. M. Hunten.